

Performance based optimal seismic retrofitting of yielding plane frames using added viscous damping

O. Lavan^{*1} and R. Levy^{2a}

¹Faculty of Civil and Environmental Engineering, Technion – Israel Institute of Technology, Haifa, Israel

²Department of Structural Engineering, Faculty of Engineering Sciences,
Ben-Gurion University of the Negev, Beer-Sheva, Israel

(Received May 24, 2010, Accepted August 8, 2010)

Abstract. This paper is concerned with the optimal seismic design of added viscous dampers in yielding plane frames. The total added damping is minimized for allowable values of local performance indices under the excitation of an ensemble of ground motions in both regular and irregular structures. The local performance indices are taken as the maximal inter-story drift of each story and/or the normalized hysteretic energy dissipated at each of the plastic hinges. Gradients of the constraints with respect to the design variables (damping coefficients) are derived, via optimal control theory, to enable an efficient first order optimization scheme to be used for the solution of the problem. An example of a ten story three bay frame is presented. This example reveals the following ‘fully stressed characteristics’ of the optimal solution: *damping is assigned only to stories for which the local performance index has reached the allowable value.* This may enable the application of efficient and practical analysis/redesign type methods for the optimal design of viscous dampers in yielding plane frames.

Keywords: supplemental viscous damping; passive control; irregular structures; yielding frames; optimal damper placement.

1. Introduction

In the 1990's seismic design codes for buildings were aimed at preventing loss of human life while permitting heavy damage to structures and property under strong earthquakes. Today damage limitation is becoming a design objective, and performance-based-design seems to emerge as the new approach to the design of earthquake resisting structures. This approach allows engineers to design structures for a desired level of seismic performance provided current codes are not violated. The new approach of performance-based-design motivates the development of new technologies and methodologies for the seismic retrofitting of existing structures, and the seismic protection of new structures. Seismic retrofitting of existing structures is often essential especially in structures that are expected to function during and after an earthquake has occurred (such as hospitals, power plants, highways and bridges).

Enhancement of the structural resistance to seismic events can be done using passive control (see

* Corresponding author, Senior Lecturer, Ph.D., E-mail: lavan@tx.technion.ac.il

^a Professor, Ph.D.

for example Soong and Dargush 1997, Christopoulos and Filiatrault 2006, Takewaki 2009). Here mechanical energy dissipation devices are installed in the structure. By dissipating energy, these devices reduce the hysteretic energy that the elements of the structure are required to dissipate and hence reduce the structural damage. The vibration energy of the structural system is appreciably reduced as well, to result in a reduction in the inter-story drifts. Of all energy dissipation devices viscous dampers seem more appropriate in the case of rehabilitation since they are velocity-dependent systems with large energy dissipations for small inter-story drifts. Moreover, the forces these velocity-dependent dampers produce are out of phase with columns axial forces and bending moments due to displacements, and therefore, will usually not require column and foundation strengthening. The third advantage of the viscous dampers is the long history of military applications that proves system reliability. Unlike metallic yielding dampers or friction dampers, viscous dampers do not result in residual internal forces due to yielding or slippage.

Initially, methodologies for the design of seismic retrofitting pre-assumed the distribution of viscous dampers throughout the building. However, Hahn and Sathiyaveeswaran, (1992) suggested that the distribution of added damping has a crucial effect on the response of the structure, thus making the need for an optimal design of these dampers, i.e. size and location, more acute. Various procedures for the allocation and distribution of viscous damping were then proposed by several researchers (Agrawal and Yang 1999, Attard 2007, Aydin *et al.* 2007, Constantinou and Tadjbakhsh 1983, Dargush and Sant 2005, Fujita *et al.* 2010, Gluck *et al.* 1996, Hwang *et al.* 2008, Kim and Bang 2002, Kim *et al.* 2003, Lavan *et al.* 2008, Lavan and Dargush 2009, Lavan and Levy 2005, 2006a, 2006b, 2009, Lee *et al.* 2005, Levy and Lavan 2006, 2009, Lin *et al.* 2008, Liu *et al.* 2004, 2005, Loh *et al.* 2000, Lopez Garcia 2001, Park *et al.* 2004, Shukla and Datta 1999, Silvestri and Trombetti 2003, 2007, Singh and Moreshchi 2001, 2002, Singh *et al.* 2003, Takewaki 1997, 2000, Takewaki and Uetani 1999, Takewaki *et al.* 1999, Trombetti and Silvestri 2004, 2005, 2007, Yang *et al.* 2002, Zhang and Soong 1992).

Takewaki (1997) proposed an approach that minimizes the sum of transfer functions' amplitudes evaluated at the natural frequency of the undamped building while constraining the total added damping. He further derived the gradients of the objective function to efficiently enable the application of first order optimization methods. Other efficient first order methods were also adopted by Lavan and Levy (2005) who derived the gradients of interstory drifts with respect to damping coefficients of added dampers. This was done in the time domain while considering a given ensemble of ground motions. The optimal designs attained by that approach led to the formulation of a simple and practical analysis/redesign scheme (Levy and Lavan, 2006). Zero-order methods were used by Zhang and Soong (1992) in their sequential search algorithm (SSA) for damping distribution and sizing. Genetic algorithms (GA) have also been used in the context of passive control optimization. Singh and Moreshchi (2002) seem to have been the first to use this approach in that context for the solution of the optimal damper distribution of viscous and viscoelastic devices. Another approach was proposed by Gluck *et al.* (1996) who presented a two stage approach that relies on optimal control theory. In the first stage, optimal active control is designed. Passive control is designed in the second stage to supply the optimal active forces attained, as adequately as possible.

Most of the abovementioned works make use of linear analysis tools that might not be valid for all structures (according to Uriz and Whittaker 2001 and Shen and Soong 1996). The validity of this assumption when it comes to cases of strength irregularities is even more questionable. Experience shows that whereas elastic analyses supply a reasonable estimation for the nonlinear behavior of

regular structures, their adequacy is questionable when it comes to irregular structures (Valmundsson and Nau 1997) due to their inability to capture the concentration of plastic hinges that usually characterizes irregular buildings. Now since the majority of buildings are irregular, nonlinear analysis tools become a must. Moreover, concentration of plastic hinges leads to a large energy dissipation demand in each of the plastic hinges, which might cause collapse if the capacity is not available.

A few methodologies were proposed for the design of viscous dampers for yielding structures (Dargush and Sant 2005, Kim *et al.* 2003, Lavan *et al.* 2008, Lavan and Dargush 2009, Lavan and Levy 2005, Shen and Soong 1996). The primary concern of the methodologies by Kim *et al.* (2003) and Shen and Soong (1996), however, was to estimate the total added damping needed rather than its distribution, while Dargush and Sant (2005) and Lavan and Dargush (2009) adopted a zero order optimization scheme that requires a large number of time history analyses. Lavan *et al.* (2008) relied on optimal control tools for nonlinear systems and proposed a methodology for attaining the optimal control forces by means of added damping and weakening structural elements. Lavan and Levy (2005) on the other hand, developed the gradients of the objective functions and constraints, hence allowed the use of an efficient first order optimization scheme. This approach, which was originally developed for yielding shear frames, is generalized in the current paper to account for general yielding plane frames with both energy constraints and drift constraints applied as design criteria. The general formulation poses new obstacles on the derivation of the solution method through optimal control theory yet allows practical use of the methodology, especially since the fully stressed characteristics of the optimal design were identified here as well.

This paper addresses the optimization problem of minimizing the total added damping of prelocated dampers subject to constraints on performance indices (such as the envelope on maximal drifts, the envelope on hysteretic energy etc.) for yielding structures excited by ensembles of realistic ground motion records. This formulation of the optimization problem is appropriate for irregular structures since local performance indices are used, and full nonlinear time history analyses are considered. An appropriate first order optimization scheme is then chosen and the required gradients of the constraints are derived.

2. Problem formulation

The formulation of the optimization problem is comprised of the total added damping as an objective function, and an inequality constraint on the upper bound of each of the local performance indices which are computed based on the behavior of the structure, i.e. satisfying the equations of motion of the damped structure. These constraints apply to each ground motion record within each ensemble. The damping coefficients which are the design variables are required to be nonnegative.

2.1 Equations of motion

The general equations of motion of a structure excited by an earthquake are usually given by

$$\mathbf{M}\ddot{\mathbf{x}}(t) + \mathbf{C}\dot{\mathbf{x}}(t) + \mathbf{f}_s(\mathbf{x}(t), \dot{\mathbf{x}}(t)) = -\mathbf{M} \cdot \mathbf{e} \cdot \mathbf{a}_g(t); \mathbf{x}(0) = \mathbf{0}, \dot{\mathbf{x}}(0) = \mathbf{0} \quad (1)$$

where \mathbf{x} = displacements vector of the degrees of freedom (DOFs); \mathbf{M} = mass matrix; \mathbf{C} = inherent

damping matrix; $\mathbf{f}_s(\mathbf{x}(t), \dot{\mathbf{x}}(t))$ = restoring forces vector; \mathbf{e} = excitation influence matrix with zero/one entries; $\mathbf{a}_g(t)$ = ground motion acceleration vector, and a dot represents differentiation with respect to the time.

The effect of plasticity is assumed to be concentrated at the edges of each element and therefore, locations of plastic hinges are defined there. It should be noted that the methodology that follows can be used for other assumptions on the plastic behavior of the structure. The behavior of these plastic hinges is assumed to follow a hysteretic rule (Fig. 1(a)) which can be decomposed into an elastic spring whose stiffness equals that of the secondary stiffness, k_α (Fig. 1(b)), and a hysteretic component with zero secondary stiffness, f_h , (Fig. 1(c)).

Thus, the behavior of each plastic hinge i can be modeled as a rotational spring with stiffness k_{ai} and an additional external moment to model f_{hi} . Fig. 1(d) presents a member having two pairs of rotational springs and restoring forces/moments in its plastic hinges.

The vector of restoring forces/moments can thus, be written as

$$\mathbf{f}_s(t) = \mathbf{K}_\alpha \mathbf{x}(t) + \mathbf{B}_{fx} \mathbf{f}_h(\mathbf{x}(t), \dot{\mathbf{x}}(t)) \quad (2)$$

where \mathbf{K}_α = secondary stiffness matrix which is actually the stiffness matrix of the structure with all plastic hinges having their rotational stiffness, k_α ; $\mathbf{f}_h(t)$ = hysteretic forces/moments vector in local coordinates of the plastic hinges with zero secondary stiffness. Since each of the plastic hinges takes a DOF in this formulation, \mathbf{B}_{fx} is a zero/one transformation matrix that ensures the correct numbering of the hinges' DOFs as will be now demonstrated.

Consider the single story frame of Fig. 1(e) where joints and plastic hinges are numbered as DOFs. Here the vector $\mathbf{f}_h(\mathbf{x}(t), \dot{\mathbf{x}}(t))$ which has 6 components at locations 4-9 is given by

$$\mathbf{f}_h(\mathbf{x}(t), \dot{\mathbf{x}}(t)) = \{f_{h,1} \ f_{h,2} \ \dots \ f_{h,6}\}^T \quad (3)$$

Matrix \mathbf{B}_{fx} which transforms these forces to the global coordinates of Fig. 1(e) is given by

$$\mathbf{B}_{fx} = \begin{bmatrix} \mathbf{0}_{3 \times 6} \\ \mathbf{I}_{6 \times 6} \end{bmatrix} \quad (4)$$

such that the product $\mathbf{B}_{fx} \mathbf{f}_h(\mathbf{x}(t), \dot{\mathbf{x}}(t))$ becomes

$$\mathbf{B}_{fx} \mathbf{f}_h(\mathbf{x}(t), \dot{\mathbf{x}}(t)) = \begin{bmatrix} \mathbf{0}_{3 \times 6} \\ \mathbf{I}_{6 \times 6} \end{bmatrix} \{f_{h,1} \ f_{h,2} \ \dots \ f_{h,6}\}^T = \{\mathbf{0}_{1 \times 3} \ f_{h,1} \ f_{h,2} \ \dots \ f_{h,6}\}^T \quad (5)$$

where $\mathbf{0}_{i \times j}$ is a zero matrix of size $i \times j$ and $\mathbf{I}_{i \times i}$ is an identity matrix of size i .

In the general case the matrix \mathbf{B}_{fx} will be of size $N \times N_{ph}$ with unit entries in the (i,j) components, where j is a plastic hinge number and i is the number of degree of freedom assigned to this plastic hinge, and zero entries elsewhere. Here N = number of DOFs and N_{ph} = number of plastic hinges.

The modeling of the vector of restoring forces/moments presented in Eq. (2) enables the formulation of the equation of motion (Eq. (1)) as follows

$$\mathbf{M}\ddot{\mathbf{x}}(t) + \mathbf{C}\dot{\mathbf{x}}(t) + \mathbf{K}_\alpha \mathbf{x}(t) + \mathbf{B}_{fx} \mathbf{f}_h(\mathbf{x}(t), \dot{\mathbf{x}}(t)) = -\mathbf{M} \cdot \mathbf{e} \cdot \mathbf{a}_g(t); \mathbf{x}(0) = \mathbf{0}, \dot{\mathbf{x}}(0) = \mathbf{0} \quad (6)$$

The constitutive laws of the hysteretic forces/moments in the elements can be formulated in

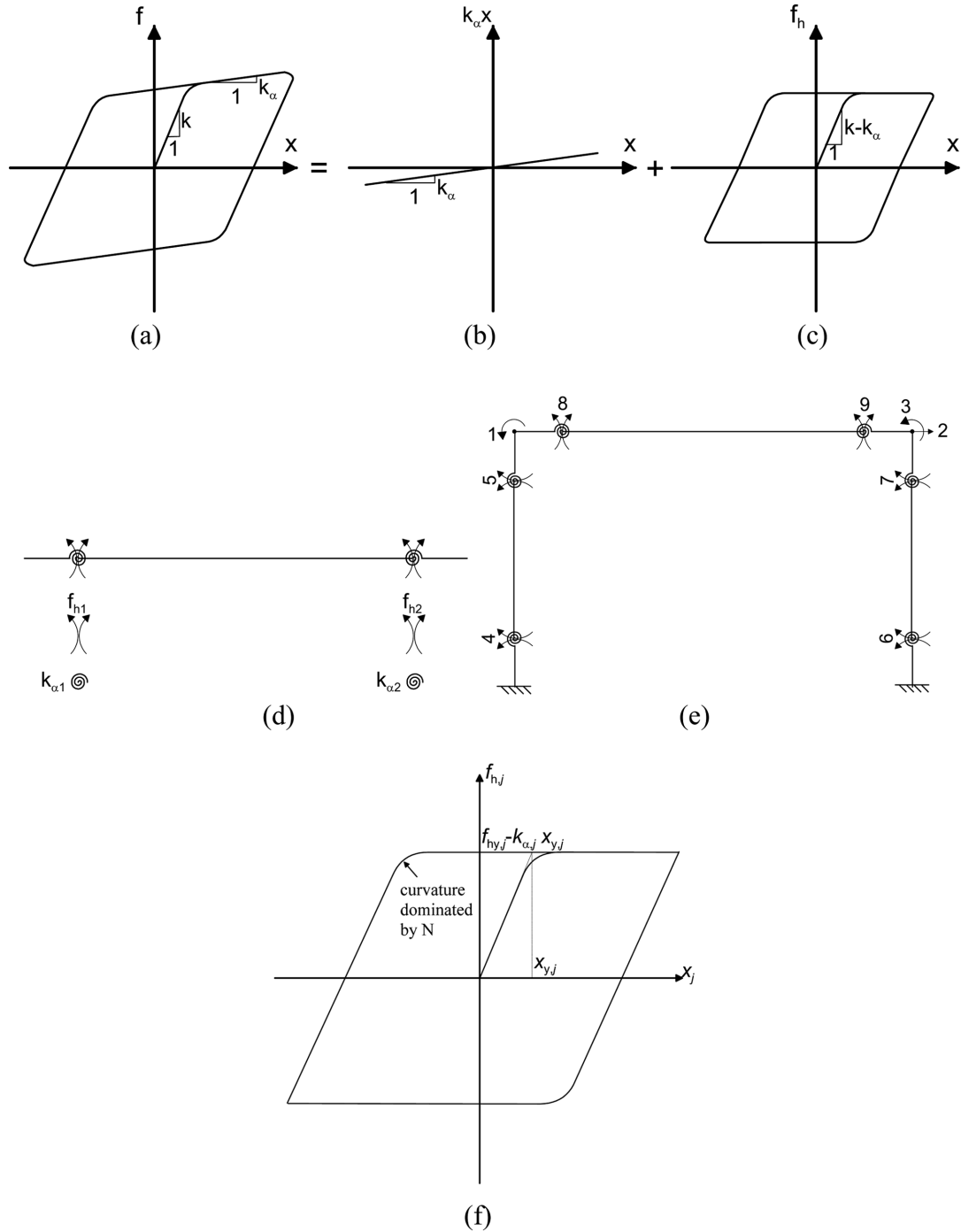


Fig. 1 (a) Total restoring force/moment, (b) elastic contribution of the secondary stiffness, (c) hysteretic contribution with zero secondary stiffness, (d) rotational spring and hysteretic components of restoring forces/moments in a single member, (e) numbering of global DOFs in a single story frame and (f) Rate independent Ozdemir model

differential form (see for example Sivaselvan and Reinhorn 2000) to yield in the following complete formulation of the equations of motion

$$\begin{aligned} \mathbf{M}\ddot{\mathbf{x}}(t) + \mathbf{C}\dot{\mathbf{x}}(t) + \mathbf{K}_\alpha \mathbf{x}(t) + \mathbf{B}_{f_x} \mathbf{f}_h(t) &= -\mathbf{M} \cdot \mathbf{e} \cdot \mathbf{a}_g(t); \mathbf{x}(0) = \mathbf{0}, \dot{\mathbf{x}}(0) = \mathbf{0} \\ \dot{\mathbf{f}}_h(t) &= \mathbf{f}(\dot{\mathbf{x}}(t), \mathbf{f}_h(t)); \mathbf{f}_h(0) = \mathbf{0} \end{aligned} \quad (7)$$

For a structure retrofitted with added damping, an additional term in the form of $\mathbf{C}_d(\mathbf{c}_d) \cdot \dot{\mathbf{x}}(t)$ is used to model the added damping effect to result in

$$\begin{aligned} \mathbf{M}\ddot{\mathbf{x}}(t) + [\mathbf{C} + \mathbf{C}_d(\mathbf{c}_d)] \cdot \dot{\mathbf{x}}(t) + \mathbf{K}_\alpha \mathbf{x}(t) + \mathbf{B}_{f_x} \mathbf{f}_h(t) &= -\mathbf{M} \cdot \mathbf{e} \cdot \mathbf{a}_g(t); \mathbf{x}(0) = \mathbf{0}, \dot{\mathbf{x}}(0) = \mathbf{0} \\ \dot{\mathbf{f}}_h(t) &= \mathbf{f}(\dot{\mathbf{x}}(t), \mathbf{f}_h(t)); \mathbf{f}_h(0) = \mathbf{0} \end{aligned} \quad (8)$$

where \mathbf{c}_d = added damping vector and $\mathbf{C}_d(\mathbf{c}_d)$ = supplemental damping matrix. This formulation of the equations of motion, and its equivalent *state space* formulation (see Soong 1990), will be used in this paper. In the *State space* formulation the equations of motion are written as

$$\begin{aligned} \dot{\mathbf{x}}(t) &= \mathbf{v}(t); \mathbf{x}(0) = \mathbf{0} \\ \dot{\mathbf{v}}(t) &= \mathbf{M}^{-1} \left(-[\mathbf{C} + \mathbf{C}_d(\mathbf{c}_d)] \cdot \mathbf{v}(t) - \mathbf{K}_\alpha \mathbf{x}(t) - \mathbf{B}_{f_x} \mathbf{f}_h(t) - \mathbf{M} \cdot \mathbf{e} \cdot \mathbf{a}_g(t) \right); \mathbf{v}(0) = \mathbf{0} \\ \dot{\mathbf{f}}_h(t) &= \mathbf{f}(\mathbf{v}(t), \mathbf{f}_h(t)); \mathbf{f}_h(0) = \mathbf{0} \end{aligned} \quad (9)$$

where \mathbf{v} = the velocity vector.

2.1.1 Hysteretic force vector

Ozdemir's rate independent model (Ozdemir 1976, see Fig. 1(f)) is adopted to model the behavior of each plastic hinge j , whose DOF is i , as

$$f_j(\dot{\mathbf{x}}(t), \mathbf{f}_h(t)) = \dot{x}_i(t) \frac{f_{hy,j} - k_{\alpha,j} x_{y,j}}{x_{y,j}} - |\dot{x}_i(t)| \frac{f_{hy,j} - k_{\alpha,j} x_{y,j}}{x_{y,j}} \left(\frac{f_{h,j}(t)}{f_{hy,j} - k_{\alpha,j} x_{y,j}} \right)^{N_j} \quad (10)$$

where $\dot{x}_i(t)$ = i -th component of $\dot{\mathbf{x}}(t)$, i.e. the velocity of the i -th degree of freedom (velocity of the relative rotation angle at the plastic hinge j); $f_{h,j}(t)$ = j -th component of $\mathbf{f}_h(t)$; f_j = j -th component of \mathbf{f} ; $f_{hy,j}$ = the yielding force of the j -th plastic hinge; $x_{y,j}$ = the yielding displacement of the j -th plastic hinge, and N_j = an odd integer. The modeling of an elastic perfectly plastic hysteresis can be achieved by assigning a large value for N_j , say 10^4+1 .

The gradient derivation, which is required for the optimization scheme and is presented in the Appendix, requires that the function $\mathbf{f}(\dot{\mathbf{x}}(t), \mathbf{f}_h(t))$ will be differentiable with respect to $\mathbf{f}_h(t)$ and $\dot{\mathbf{x}}(t)$. This requirement is met by replacing the $|\dot{x}|$ in Ozdemir's rate independent model, which is used here, with $\dot{x} \cdot \text{sign}(\dot{x}) \approx \dot{x} \cdot \dot{x} / (|\dot{x}| + \delta)$ where δ = a small number, say 0.01. Thus, for the j -th plastic hinge, having a degree of freedom is i , the function f_j becomes

$$f_j(\dot{\mathbf{x}}(t), \mathbf{f}_h(t)) = \dot{x}_i(t) \frac{f_{hy,j} - k_{\alpha,j} x_{y,j}}{x_{y,j}} \left(1 - \frac{\dot{x}_i(t)}{|\dot{x}_i(t)| + \delta_j} \left(\frac{f_{h,j}(t)}{f_{hy,j} - k_{\alpha,j} x_{y,j}} \right)^{N_j} \right) \quad (11)$$

2.2 Performance indices as constraints

Two local performance indices are chosen in this paper: the hysteretic energy dissipated by each of the plastic hinges and the maximal inter-story drifts. Other performance indices, such as the Park and Ang (1985) damage index, can be easily implemented using the methodology that follow. These performance indices are normalized by given allowable values so that a value of unity indicates that a performance index reached its allowable value.

The hysteretic energy accumulated in plastic hinge i (Uang and Bertero 1990), normalized by its allowable value, is given by

$$E_{h,i}(t_f) = \frac{\int_0^{t_f} f_{h,i}(t) \cdot v_i(t) dt}{E_{h,i}^{all}} \quad (12)$$

where t_o = the initial time of the excitation; t_f = the final time of the excitation\computation; $E_{h,i}(t_f)$ = normalized hysteretic energy at the plastic hinge i at the time t_f ; $f_{h,i}(t)$ = hysteretic force/moment in the plastic hinge i ; $v_i(t)$ = velocity of the degree of freedom associated with the plastic hinge i , and $E_{h,i}^{all}$ = allowable value of the hysteretic energy at the plastic hinge i .

The performance constraint on the hysteretic energy in the plastic hinges, in vector form, becomes

$$\mathbf{E}_h(t_f) = \mathcal{D}^{-1}(\mathbf{E}_h^{all}) \cdot \int_0^{t_f} \mathcal{D}(\mathbf{f}_h(t)) \cdot (\mathbf{B}_{xf} \dot{\mathbf{x}}(t)) dt \leq \mathbf{1} \quad (13)$$

where $\mathcal{D}(\mathbf{z})$ = operator that forms a diagonal matrix whose diagonal elements are the elements of a given vector \mathbf{z} , $\mathbf{1}$ = unit vector and \mathbf{E}_h^{all} = vector of allowable values of hysteretic energies at the plastic hinges and $\mathbf{B}_{xf} = \mathbf{B}_{fx}^T$ = a matrix that transforms the velocities from the general DOFs to plastic hinges.

In addition, a performance constraint on the normalized maximal inter-story drifts is considered. This constraint can be written as

$$\mathbf{d}_m = \max_t \left(\text{abs} \left(\mathcal{D}^{-1}(\mathbf{d}^{all}) \cdot \mathbf{H}_x \mathbf{x}(t) \right) \right) \quad (14)$$

where \mathbf{d}_m = vector of normalized maximal inter-story drifts; \mathbf{d}^{all} = vector of allowable maximal inter-story drifts; \mathbf{H}_x = transformation matrix that transforms the displacements from the global coordinates of the DOFs to the coordinates of inter-story drifts, and “abs” stands for the absolute function as it acts on each of the vector components separately. For the single story of Fig. 1(e), for example, the inter-story drift to be controlled is actually the relative displacement of the DOF 2 to the ground. Here matrix \mathbf{H}_x becomes

$$\mathbf{H}_x = [0 \ 1 \ 0_{1 \times 7}] \quad (15)$$

In order to reduce the number of constraints, hence the number of gradients to be derived and computed, they are replaced by a single constraint on p_i , a *performance index* that considers the maximal value of all components of the normalized hysteretic energy and the normalized drift vectors. It is presented as

$$pi = \max(\max(\mathbf{E}_h(t_f)), \max(\mathbf{d}_m)) \leq 1.0 \quad (16)$$

2.3 Problem formulation

The formal *state space* formulation of the optimization problem may now be formulated as

$$\left. \begin{aligned} &\text{minimize: } J = \mathbf{c}_d^T \cdot \mathbf{1} \\ &\text{subject to:} \\ &pi = \max(\max(\mathbf{E}_h(t_f)), \max(\mathbf{d}_m)) \leq 1.0 \\ &\text{where} \\ &\dot{\mathbf{E}}_h(t) = \mathcal{D}^{-1}(\mathbf{E}_h^{all}) \cdot \mathcal{D}(\mathbf{f}_h(t)) \cdot (\mathbf{B}_{xf} \mathbf{v}(t)) ; \mathbf{E}_h(0) = \mathbf{0} \\ &\dot{\mathbf{d}}_{m,p} = \frac{1}{t_f} (\mathcal{D}^{-1}(\mathbf{d}^{all}) \cdot \mathcal{D}(\mathbf{H}_x \cdot \mathbf{x}(t)))^p \cdot \mathbf{1} ; \mathbf{d}_{m,p}(0) = \mathbf{0} \\ &\text{and } \mathbf{x}(t), \mathbf{v}(t) \text{ and } \mathbf{f}_h(t) \text{ satisfy the equations of motion} \\ &\dot{\mathbf{x}}(t) = \mathbf{v}(t) ; \mathbf{x}(0) = \mathbf{0} \\ &\dot{\mathbf{v}}(t) = \mathbf{M}^{-1}(-[\mathbf{C} + \mathbf{C}_d(\mathbf{c}_d)] \cdot \mathbf{v}(t) - \mathbf{K}_\alpha \mathbf{x}(t) - \mathbf{B}_{fx} \mathbf{f}_h(t) - \mathbf{M} \cdot \mathbf{e} \cdot \mathbf{a}_g(t)) ; \mathbf{v}(0) = \mathbf{0} \\ &\dot{\mathbf{f}}_h(t) = \mathbf{f}(\mathbf{v}(t), \mathbf{f}_h(t)) ; \mathbf{f}_h(0) = \mathbf{0} \\ &\mathbf{0} \leq \mathbf{c}_d \leq \mathbf{c}_{d,max} \end{aligned} \right\} \forall \mathbf{a}_g \in \text{ensemble } i \quad (17)$$

where *ensemble* i = the i -th ensemble of ground motions and $\mathbf{c}_{d,max}$ = upper bound on \mathbf{c}_d . If more than one ensemble is to be considered, with different intensities and different allowable drifts and energies, the constraints are repeated for all the ensembles. Ensembles that represent a short return period will then receive smaller allowable values for the drifts and energies.

3. Optimization scheme

Solution of an optimization problem using zero order optimization schemes, i.e. without using gradients, usually requires a large number of function and constraints evaluations. For the problem at hand, the evaluation of the constraints is computationally expensive, hence use is made of a first order optimization scheme, which requires evaluation of the gradients of the objective function and the constraints with respect to the design variables (damping coefficients). Those are presented in the Appendix. In this paper the cutting planes method is adopted due to the “flat” nearly convex behavior of the constraints. At each iteration, the actual nonlinear objective function and constraints are linearized to result in a linear programming problem which can be easily solved using common existing methods. The gradients of the objective function and the constraints are required for the linearization process at each iteration. Thus the solution requires a time history analysis for each record (constraint) at every iteration cycle. In order to reduce the computational effort, optimization is first carried out for one “active” ground motion (loading condition), to be subsequently defined, rather than for the whole ensemble. If the optimal solution for this ground motion violates other records in the ensemble, additional ground motions are added one at a time (*Stage 4* below). Following are the main stages of the optimization scheme, as will be elaborated subsequently:

Stage 1: Select the “active” ground motion.

Stage 2: Compute an initial starting value for the damping vector.

Stage 3: Solve the optimization problem for the active set of records using the Cutting Planes Method.

Stage 4: Perform an analysis using the attained optimal set of design variables for each of the remaining records in the ensemble for a feasibility check and return to *Stage 3* if additional ground motion is added to the active set.

Stage 5: Stop.

Stage 1: Selection of the “active” ground motion record

A good selection of the starting ground motion is one for which the starting ground motion remains active at the optimum. In this work, since displacements and energies are constrained, the record with the maximal displacement or input energy, is selected to begin the process, depending on which of the two is expected to be dominant. The displacement and input energy are evaluated from a SDOF having the fundamental period of the undamped structure within the expected total damping ratio range.

Stage 2: Computation of a starting point, \mathbf{c}_{do}

The starting point is evaluated by first assuming a distribution for the damping vector. This damping vector can be evaluated using any of the approximate methods from the literature (for example Hahn and Sathiyageeswaran 1992, or Kim *et al.* 2003), or more simply by assuming equal damping for all dampers, as was done in this work. Then this damping vector is multiplied by a factor that is obtained iteratively using the Secant Method so as to satisfy

$$pi = 1.0 \quad (18)$$

where pi in Eq. (18) is computed from a time history analysis of the frame excited by the “active” ground motion of *Stage 1*.

Stage 3: Solution of the optimization problem

Optimization technique of the optimization problem

The gradients of the constraint that are essential for the *cutting planes* method are calculated using the gradient derivation technique which is described in the Appendix. If more than one record is “active”, say two, then the gradients of the constraints associated with these two records, and thus the linear equivalent constraints, are calculated separately for each record using the same technique of gradient evaluation to result in a linear programming problem with double the number of constraints.

Maximum step size: The step size proposed for the Cutting Planes Method is the total damping divided by a factor ρ . Instead of using a circle of radius r , (in the 2-dimensional space) for the step size, a square of side $r/\sqrt{2}$, is used. This results in linear side constraints for the step size. In the n -dimensional space, r/\sqrt{n} is taken in place of $r/\sqrt{2}$.

Constraints elimination: Since the Cutting Planes Method is not appropriate for non-convex problems a modification is needed. The modification is as follows: if the nonlinear constraint at iteration j is satisfied yet not active and its linear counterpart at iteration i for $i < j$, is satisfied and active, then that plane is removed from the next iteration. If not removed, these linear constraints will cut the feasible region.

Stage 4: time history analyses

At this stage, a time history analysis is performed on the optimally damped structure for each of the remaining records in the ensemble, separately. A new candidate ground motion to be considered as active is the one with the largest pi . It is actually added to the active set only if its pi is larger than 1.0.

In the examples to follow two records at most are active. These records are easily tracked by the algorithm, and it is expected that the optimization scheme is likely to use, in general only a few of the records and not a whole ensemble. Therefore, the scheme becomes practical in the sense of the computational effort.

Stage 5: Termination decision

The methodology is terminated if no additional ground motion is added to the active set.

4. Example

This example adopts the 10 story 3 bay industrial building that was used by Levy and Lavan (2006), who solved the optimization problem for the drifts' constraints only, assuming linear behavior of the damped frame. This time, however, a nonlinear analysis is considered. For the sake of comparison with Levy and Lavan (2006), axial deformations are neglected, i.e. vertical restraints are assigned to all joints, and the horizontal degrees of freedom of each floor are slaved to one of the horizontal degrees of freedom at that floor using rigid links technique. The dampers in this example are installed on diagonals rather than using chevron braces, i.e. the dampers are not horizontal.

Design variables were assigned to each of the dampers and none were a priori, assumed equal. The ground motion ensemble was chosen as the "SE 10% in 50 years" ensemble (Somerville *et al.* 1997) and the allowable drift was chosen as 1.0%.

Drift control: The maximal displacement obtained using time history analysis of a single degree of freedom structure for which the period is 2.6 sec, which is the fundamental period of the 10 story frame, was plotted by Levy and Lavan (2006) versus the damping ratio, for each of the records within the ensemble separately (*Stage 1* of the optimization scheme). The record SE01 led to the largest spectral displacement for the fundamental period of the structure (see Levy and Lavan 2006), hence it should have been chosen to start the process (*Stage 1* of the optimization scheme). However, in view of the results obtained by Levy and Lavan (2006), both records SE01 and SE19 were chosen to start the process.

Equal starting values for the dampers were obtained using the procedure given in *Stage 2* of the optimization scheme. These starting values sum to a total damping of $100000 \text{ kN} \cdot \text{s/m}$. Allowable drifts are taken as 1%.

Proceeding with *Stage 3* of the optimization scheme, Fig. 2(a) shows the optimal damping and maximum drifts of the damped frame excited by SE01 and SE19.

Having calculated the optimal damping for these two records, a nonlinear time history analysis was performed on the optimally damped structure for each of the remaining 18 records (*Stage 4* of the optimization scheme). Since no other record led to higher inter-story drifts than the allowed, there was no record to be added to the active set and the process was terminated.

A comparison of Fig. 2(a) with the results presented by Levy and Lavan (2006) for the linear case

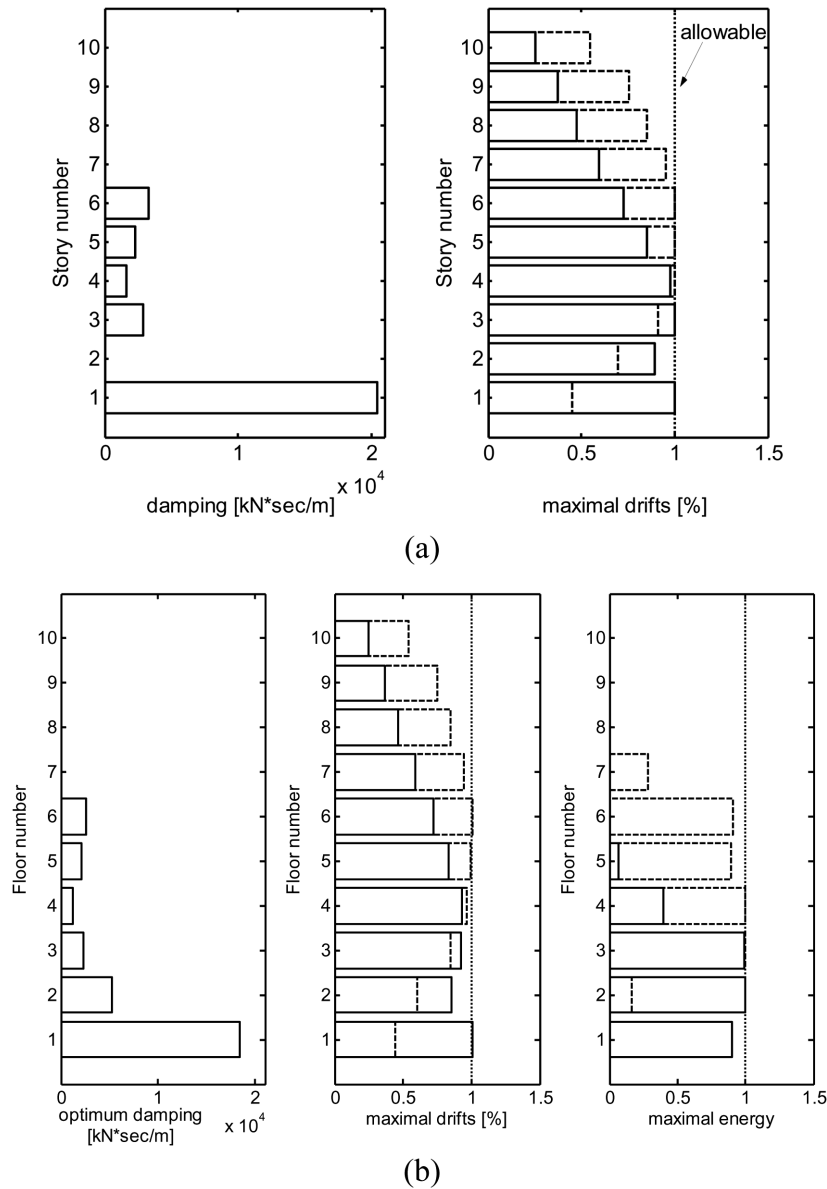


Fig. 2 (a) case I: Optimal supplemental damping (left) and drifts envelope for the optimally damped frame excited by the SE 10 % in 50 years ensemble (on the right, SE01 – continuous line, and SE19 – dashed line) and (b) case II: optimal damping, normalized drift and normalized hysteretic energy at the plastic hinges for the SE01 (continuous line), and SE19 (dashed line) records

(not shown here) shows that, here too, drifts of the same five stories are fully utilized, i.e. reached the allowable drift, and the rest of the drifts are smaller than the allowable. Again, these stories are the only stories with assigned damping at the optimum. Note that the orientation of the added damping in the linear (Levy and Lavan 2006) case was horizontal, hence, if comparison is done, the added damping of the nonlinear case should be multiplied by $\cos^2 \alpha = 5^2 / (5^2 + 3^2) = 25/34$. The total

added damping in the optimal solution sums up to $30588 \text{ kN} \cdot \text{s/m}$.

Drift and energy control: This frame is further investigated by limiting the hysteretic energy dissipated at each of the plastic hinges, divided by two times its elastic energy at yielding, to an allowable value of 2.5. Again, the records SE01 and SE19 are chosen to begin the process. A total damping of $100000 \text{ kN} \cdot \text{s/m}$ was equally distributed in the ten dampers to result in the starting point for the Cutting Planes Method of *Stage 3* of the optimization scheme. The optimization scheme was then executed and 20 iterations were practically sufficient to reach the optimal design.

The optimal damping, normalized inter-story drifts and normalized hysteretic energy of each story (i.e. maximal in its columns and beams) for the records SE01 and SE19 are plotted in Fig. 2(b). It should be noted that the beams in the central bays had the maximal normalized hysteretic energy at each story while columns did not yield at all.

Stage 4 of the optimization scheme revealed that no other record within the ensemble resulted in larger inter-story drifts or normalized hysteretic energies than the allowed, hence the damping of Fig. 2(b) is the optimal damping for the whole ensemble. As can be seen from Fig. 2(b), dampers are assigned to the first six stories while each of these stories reached either the allowable inter-story drift or allowable normalized hysteretic energy. The total added damping in the optimal solution sums up to $31905 \text{ kN} \cdot \text{s/m}$ and is a bit larger than the total added damping in the optimal solution where only drifts were constrained, as expected.

5. Conclusions

A gradient based methodology for the optimal design of added viscous damping for an ensemble of realistic ground motion records with constraints on the maximum inter-story drifts and on maximum energy based local damage indices for nonlinear frames, was presented. This approach for the optimal seismic design of added viscous damping in framed structures was used for the solution of the optimization problem for nonlinear plane frames. Because local performance indices are constrained, the formulation is appropriate for use both cases where regular structures and irregular structures are considered.

The gradients of the constraints were derived so as to enable the use of an efficient first order optimization scheme for the solution of the optimization problem. Since the constraints depend on the added damping vector through differential equations (the equations of motion), the derivation of these gradients required reformulation of the optimization problem, as well as the use of variational calculus.

The optimal design of the yielding plane frames studied in this work, with drift constraints, possesses the same fully stressed behavior observed by Levy and Lavan (2006) for the linear case. Here too, stories having supplemental damping at the optimum reached allowable drifts. Moreover, for energy constraints, the optimal design assigns added damping in the stories below the fully stressed beams. In the general case of constraining both drifts and energies:

The optimal design assigns dampers where either the drifts or the energies reach pre-assigned allowable values.

This may enable the application of efficient and practical analysis/redesign type methods (e.g. Levy and Lavan 2006) for the optimal design of viscous dampers in yielding plane frames.

References

- Agrawal, A.K. and Yang, J.N. (1999), "Design of passive energy dissipation systems based on LQR control methods", *J. Intel. Mat. Syst. Str.*, **10**(12), 933-944.
- Agrawal, A.K. and Yang, J.N. (1999), "Optimal placement of passive dampers on seismic and wind-excited buildings using combinatorial optimization", *J. Intel. Mat. Syst. Str.*, **10**(12), 997-1014.
- Attard, T.L. (2007), "Controlling all interstory displacements in highly nonlinear steel buildings using optimal viscous damping", *J. Struct. Eng.*, **133**(9), 1331-1340.
- Aydin, E., Boduroglu, M.H. and Guney, D. (2007), "Optimal damper distribution for seismic rehabilitation of planar building structures", *Eng. Struct.*, **29**, 176-185.
- Christopoulos, C. and Filiatrault, A. (2006), *Principles of supplemental damping and seismic isolation*, Milan, Italy, IUSS Press.
- Constantinou, M.C. and Tadjbakhsh, I.G. (1983), "Optimum design of a first story damping system", *Comput. Struct.*, **17**(2), 305-310.
- Dargush, G.F. and Sant, R.S. (2005), "Evolutionary aseismic design and retrofit of structures with passive energy dissipation", *Earthq. Eng. Struct. Dyn.*, **34**, 1601-1626.
- fujita, k., moustafa, a. and takewaki, i. (2010), optimal placement of viscoelastic dampers and supporting members under variable critical excitations. *Earthq. Struct.*, **1**(1), 43-67.
- Gluck, N., Reinhorn, A.M., Gluck, J. and Levy, R. (1996), "Design of supplemental dampers for control of structures", *J. Struct. Eng. - ASCE*, **122**(12), 1394-1399.
- Hahn, G.D. and Sathiyaveeswaran, K.R. (1992), "Effects of added-damper distribution on the seismic response of buildings", *Comput. Struct.*, **43**(5), 941-950.
- Hwang, J.S. and Huang, Y.N. et al. (2008), "Design formulations for supplemental viscous dampers to building structures", *J. Struct. Eng.*, **134**(1), 22-31.
- Kim, J. and Bang, S. (2002), "Optimum distribution of added viscoelastic dampers for mitigation of torsional responses of plan-wise asymmetric structures", *Eng. Struct.*, **24**(10), 1257-1269.
- Kim, J., Choi, H. and Min, K.W. (2003), "Performance-based design of added viscous dampers using capacity spectrum method", *J. Earthq. Eng.*, **7**(1), 1-24.
- Lavan, O., Cimellaro, G.P. and Reinhorn, A.M. (2008), "Noniterative optimization procedure for seismic weakening and damping of inelastic structures", *J. Struct. Eng.*, **134**(10), 1638-1648.
- Lavan, O. and Dargush, G.F. (2009), "Multi-objective optimal seismic retrofitting of structures", *J. Earthq. Eng.*, **13**, 758-790.
- Lavan, O. and Levy, R. (2005), "Optimal design of supplemental viscous dampers for irregular shear-frames in the presence of yielding", *Earthq. Eng. Struct. Dyn.*, **34**, 889-907.
- Lavan, O. and Levy, R. (2006a), "Optimal design of supplemental viscous dampers for linear framed structures", *Earthq. Eng. Struct. Dyn.*, **35**, 337-356.
- Lavan, O. and Levy, R. (2006b), "Optimal peripheral drift control of 3D irregular framed structures using supplemental viscous dampers", *J. Earthq. Eng.*, **10**(6), 903-923.
- Lavan, O. and Levy, R. (2009), "Simple iterative use of Lyapunov's solution for the linear optimal seismic design of passive devices in framed buildings", *J. Earthq. Eng.*, **13**(5), 650-666.
- Levy, R. and Lavan, O. (2006), "Fully stressed design of passive controllers in framed structures for seismic loadings", *J. Struct. Multidiscip. O.*, **32**(6), 485-498.
- Levy, R. and Lavan, O. (2009), "Quantitative comparison of optimization approaches for the design of supplemental damping in earthquake engineering practice", *J. Struct. Eng.*, **135**(3), 321-325.
- Lin, Y.Y., Chang, K.C. and Chen, C.Y. (2008), "Direct displacement-based design for seismic retrofit of existing buildings using nonlinear viscous dampers", *Bull. Earthq. Eng.*, **6**, 535-552.
- Liu, W., Tong, M. and Lee, G.C. (2005), "Optimization methodology for damper configuration based on building performance indices", *J. Struct. Eng.*, **131**(11), 1746-1756.
- Liu, W., Tong, M., Wu, Y. and Lee, G.C. (2004), "Optimized damping device configuration design of a steel frame structure based on building performance indices", *Earthq. Spectra*, **20**(1), 67-89.
- Loh, C.H., Lin, P.Y. and Chung, N.H. (2000), "Design of dampers for structures based on optimal control theory", *Earthq. Eng. Struct. Dyn.*, **29**(9), 1307-1323.

- Lopez-Garcia, D. (2001) "A simple method for the design of optimal damper configurations in MDOF structures", *Earthq. Spectra*, **17**(3), 387-398.
- Ozdemir, H. (1976), *Nonlinear transient dynamic analysis of yielding structures*, Ph. D. dissertation, University of California, Berkeley.
- Park, Y.J. and Ang, A.H.S. (1985), "Mechanistic seismic damage model for reinforced concrete", *J. Struct. Eng.*, **111**(4), 722-739.
- Park, J.H. kim, J. and Min, K.W. (2004), "Optimal design of added viscoelastic dampers and supporting braces", *Earthq. Eng. Struct. Dyn.*, **33**, 465-484.
- Shen, K.L. and Soong, T.T. (1996), "Design of energy dissipation devices based on concept of damage control", *J. Struct. Eng. - ASCE*, **122**(1), 76-82.
- Shukla, A.K. and Datta, T.K. (1999), "Optimal use of viscoelastic dampers in building frames for seismic force", *J. Struct. Eng. - ASCE*, **125**(4), 401-409.
- Silvestri, S. and Trombetti, T. (2007), "Physical and numerical approaches for the optimal insertion of seismic viscous dampers in shear-type structures", *J. Earthq. Eng.*, **11**(5), 787-828.
- Silvestri, S., Trombetti, T. and Ceccoli, C. (2003), "Inserting the mass proportional damping (MPD) system in a concrete shear-type structure", *Struct. Eng. Mech.*, **16**(2), 177-193.
- Singh, M.P. and Moreschi, L.M. (2001), "Optimal seismic response control with dampers", *Earthq. Eng. Struct. Dyn.*, **30**(4), 553-572.
- Singh, M.P. and Moreschi, L.M. (2002), "Optimal placement of dampers for passive response control", *Earthq. Eng. Struct. Dyn.*, **31**(4), 955-976.
- Singh, M.P. Verma, N.P. and Moreschi, L.M. (2003), "Seismic analysis and design with Maxwell dampers", *J. Eng. Mech.*, **129**(3), 273-282.
- Sivaselvan, M.V. and Reinhorn, A.M. (2000), "Hysteretic models for deteriorating structures", *J. Eng. Mech. - ASCE*, **126**, 633-640.
- Somerville, P., Smith, N., Punyamurthula, S. and Sun, J. (1997), "Development of ground motion time histories for Phase 2 of the FEMA/SAC steel project", Report No. SAC/BD-97/04. The ground motions can be downloaded from: "http://quiver.eerc.berkeley.edu:8080/studies/system/ground_motions.html".
- Soong, T.T. (1990), *Active structural control*, Longman Scientific & Technical, Harlow, England.
- Soong, T.T. and Dargush, G.F. (1997), *Passive energy dissipation systems in structural engineering*, John Wiley & Sons Ltd., Chichester.
- Takewaki, I. (1997), "Optimal damper placement for minimum transfer function", *Earthq. Eng. Struct. Dyn.*, **26**(11), 1113-1124.
- Takewaki, I. (2000), "Optimal damper placement for critical excitation", *Probabilist. Eng. Mech.*, **15**(4), 317-325.
- Takewaki, I. (2000), "Optimal damper placement for planar building frames using transfer functions", *Struct. Multidiscip. O.*, **20**(4), 280-287.
- Takewaki, I. and Uetani, K. (1999), "Optimal damper placement for building structures including surface ground amplification", *Soil Dyn. Earthq. Eng.*, **18**(5), 363-371.
- Takewaki, I. Yoshitomi, S. Uetani, K. and Tsuji, M. (1999), "Non-monotonic optimal damper placement via steepest direction search", *Earthq. Eng. Struct. Dyn.*, **28**(6), 655-670.
- Takewaki, I. (2009), *Building control with passive dampers: optimal performance-based design for earthquakes*, John Wiley & Sons Ltd. (Asia), Singapore.
- Trombetti, T. and Silvestri, S. (2004), "Added viscous dampers in shear-type structures: the effectiveness of mass proportional damping", *J. Earthq. Eng.*, **8**(2), 275-313.
- Trombetti, T. and Silvestri, S. (2006), "On the modal damping ratios of shear-type structures equipped with Rayleigh damping systems", *J. Sound Vib.*, **292**, 21-58.
- Trombetti, T. and Silvestri, S. (2007), "Novel schemes for inserting seismic dampers in shear-type systems based upon the mass proportional component of the Rayleigh damping matrix", *J. Sound Vib.*, **302**(3), 486-526.
- Uang, C.M. and Bertero, V.V. (1990), "Evaluation of seismic energy in structures", *Earthq. Eng. Struct. Dyn.*, **19**(1), 77-90.
- Uriz, P. and Whittaker, A.S. (2001), "Retrofit of pre-Northridge steel moment-resisting frames using fluid viscous dampers", *Struct. Design Tall Build.*, **10**, 371-390.
- Valmundsson, V.E. and Nau, J.M. (1997), "Seismic response of building frames with vertical structural

- irregularities”, *J. Struct. Eng. - ASCE*, **123**(12), 30-41.
- Yang, J.N., Lin, S., Kim, J.H. and Agrawal, A.K. (2002), “Optimal design of passive energy dissipation systems based on H infinity and H2 performances”, *Earthq. Eng. Struct. Dyn.*, **31**(4), 921-936.
- Zhang, R.H. and Soong, T.T. (1992), “Seismic design of viscoelastic dampers for structural applications”, *J. Struct. Eng. - ASCE*, **118**(5), 1375-13

IT

Appendix: A differentiable equivalent to the constraint

Before proceeding formally with the gradient derivation for its solution, it is obvious that pi in Eq. (17) will pose an obstacle since use is made of a variational approach. This difficulty is overcome by replacing the max function on t in Eq. (14) with a differentiable function. It is proposed to use a norm of the p -type differentiable function as an equivalent to $\mathbf{d}_m = \max_t(\text{abs}(\mathcal{D}^{-1}(\mathbf{d}^{all}) \cdot \mathbf{H}_x \mathbf{x}(t)))$. Thus, \mathbf{d}_m takes the form of

$$\mathbf{d}_m(t_f) = \left(\frac{1}{t_f} \int_0^{t_f} (\mathcal{D}^{-1}(\mathbf{d}^{all}) \cdot \mathcal{D}(\mathbf{H}_x \cdot \mathbf{x}(t)))^p dt \right)^{\frac{1}{p}} \cdot \mathbf{1} = (\mathcal{D}(\mathbf{d}_{m,p}(t_f)))^{\frac{1}{p}} \cdot \mathbf{1} \quad (\text{A.1})$$

where p = a large positive even number and

$$\mathbf{d}_{m,p}(t_f) = (\mathcal{D}(\mathbf{d}_m))^p \cdot \mathbf{1} = \frac{1}{t_f} \int_0^{t_f} (\mathcal{D}^{-1}(\mathbf{d}^{all}) \cdot \mathcal{D}(\mathbf{H}_x \cdot \mathbf{x}(t)))^p dt \cdot \mathbf{1} \quad (\text{A.2})$$

Since the gradient derivation requires that the equations of motion and the relations defining $\mathbf{d}_{m,p}$ be formulated as a set of first order differential equations, Eq. (A.2) can be differentiated with respect to time to result in

$$\dot{\mathbf{d}}_{m,p} = \frac{1}{t_f} (\mathcal{D}^{-1}(\mathbf{d}^{all}) \cdot \mathcal{D}(\mathbf{H}_x \cdot \dot{\mathbf{x}}(t)))^p \cdot \mathbf{1} \quad ; \quad \mathbf{d}_{m,p}(0) = \mathbf{0} \quad (\text{A.3})$$

and its value at t_f will be constrained. The use of *state space* notation requires the differentiation of the constraint on the normalized hysteretic energy as well, to yield

$$\dot{\mathbf{E}}_h(t) = \mathcal{D}^{-1}(\mathbf{E}_h^{all}) \cdot \mathcal{D}(\mathbf{f}_h(t)) \cdot (\mathbf{B}_{xf} \dot{\mathbf{x}}(t)) \quad ; \quad \mathbf{E}_h(0) = \mathbf{0} \quad (\text{A.4})$$

And again, its value at t_f will be constrained. The maximal component of a vector with non-negative entries, \mathbf{z} , can be evaluated using a differentiable weighted average of the form

$$z_{max} = \frac{\sum w_i^q z_i}{\sum w_i^q} \quad (\text{A.5})$$

where w_i = weight of z_i and q = an index. When q is large, say $q = p$, and the components of \mathbf{z} are used as their own weights, i.e. $w_i = z_i$, this weighted average approaches the value of the maximum component of \mathbf{z} . Since $\mathbf{E}_h(t_f)$ and are normalized quantities pi can be written as $p_i = \max(\mathbf{E}_h(t_f), \mathbf{d}_m)$ and reformulate pi in Eq. (17) as

$$pi = \frac{\mathbf{1}^T \cdot \mathcal{D}^{q+1}(\mathbf{E}_h(t_f)) \cdot \mathbf{1} + \mathbf{1}^T \cdot \mathcal{D}^{q+1}(\mathbf{d}_m) \cdot \mathbf{1}}{\mathbf{E}_h(t_f) \cdot \mathcal{D}^q(\mathbf{E}_h(t_f)) \cdot \mathbf{1} + \mathbf{1}^T \cdot \mathcal{D}^q(\mathbf{d}_m) \cdot \mathbf{1}} \quad (\text{A.6})$$

Substituting Eq. (A.1) yields

$$pi = \frac{\mathbf{1}^T \cdot \mathcal{D}^{q+1}(\mathbf{E}_h(t_f)) \cdot \mathbf{1} + \mathbf{1}^T \cdot \mathcal{D}^{\frac{q+1}{p}}(\mathbf{d}_{m,p}(t_f)) \cdot \mathbf{1}}{\mathbf{1}^T \cdot \mathcal{D}^q(\mathbf{E}_h(t_f)) \cdot \mathbf{1} + \mathbf{1}^T \cdot \mathcal{D}^{\frac{q}{p}}(\mathbf{d}_{m,p}(t_f)) \cdot \mathbf{1}} \quad (\text{A.7})$$

Gradient derivation using a variational approach

The evaluation of the gradient of the objective function is trivial since this function depends on the design variables explicitly, and is given by $\nabla_{c_d} j = \mathbf{1}$. The evaluation of the gradient of the constraints, however, is not that trivial since the constraints do not depend on the design variables explicitly but on the design variables through differential equations.

The gradient derivation in this paper is achieved indirectly by formulating the problem in *state space* notation and using a variational approach.

Eq. (24) has the general form of

$$\begin{aligned} & \text{minimize } f(\mathbf{c}_d) \\ & \text{subject to: } g(\mathbf{y}(t_f)) - g_{max} \leq 0 \\ & \text{where } \dot{\mathbf{y}}(t) = \mathbf{a}(\mathbf{y}(t), \mathbf{c}_d, t) \quad ; \quad \mathbf{y}(t_o) = \mathbf{0} \end{aligned} \quad (\text{A.8})$$

where $\mathbf{y} = \{\mathbf{E}_h \mathbf{d}_{m,p} \mathbf{x} \mathbf{v} \mathbf{f}_h\}^T$. The gradient of $g(\mathbf{y}(t_f))$ is obtained from the following formulation of the constraint

$$\begin{aligned} & g(\mathbf{y}(t_f)) \\ & \text{where } \mathbf{y}(t) \text{ satisfies} \\ & \dot{\mathbf{y}}(t) = \mathbf{a}(\mathbf{y}(t), \mathbf{c}_d, t) \quad ; \quad \mathbf{y}(t_o) = \mathbf{0} \end{aligned} \quad (\text{A.9})$$

or equivalently

$$\begin{aligned} & \int_{t_o}^{t_f} \frac{dg(\mathbf{y}(t))}{dt} dt + g(\mathbf{y}(t_o)) \\ & \text{where } \mathbf{y}(t) \text{ satisfies } \dot{\mathbf{y}}(t) = \mathbf{a}(\mathbf{y}(t), \mathbf{c}_d, t) \quad ; \quad \mathbf{y}(t_o) = \mathbf{0} \end{aligned} \quad (\text{A.10})$$

for which the augmented function is given by

$$J_a = \int_{t_o}^{t_f} \left[\frac{dg(\mathbf{y}(t))}{dt} + \boldsymbol{\lambda}^T(t) [\mathbf{a}(\mathbf{y}(t), \mathbf{c}_d, t) - \dot{\mathbf{y}}(t)] \right] dt + g(\mathbf{y}(t_o)) \quad (\text{A.11})$$

where $\boldsymbol{\lambda} = \{\boldsymbol{\lambda}_{Eh}^T \boldsymbol{\lambda}_{dmp}^T \boldsymbol{\lambda}_x^T \boldsymbol{\lambda}_v^T \boldsymbol{\lambda}_{fh}^T\}^T$. Note that the value of the constraint at $t = t_o$ is zero, i.e. $g(\mathbf{y}(t_o)) = 0$. Applying the chain rule on the first term on the right hand side of Eq. (A.11) and taking the variation of this augmented function, with both t_o and t_f specified, is first taken. Then, integration by parts is applied to the term in which the variation on $\dot{\mathbf{y}}(t)$ appears. This leads to the following expression for the variation of the augmented function

$$\begin{aligned}
\delta J_a(\mathbf{c}_d) = & \left[\left[\frac{\partial g(\mathbf{y}(t))}{\partial \mathbf{y}} - \boldsymbol{\lambda}(t) \right]^T \cdot \delta \mathbf{y} \right]_{t_f} \\
& + \int_{t_o}^{t_f} \left[\left[\frac{\partial}{\partial \mathbf{y}} (\boldsymbol{\lambda}^T(t) \cdot \mathbf{a}(\mathbf{y}(t), \mathbf{c}_d, t)) + \frac{d\boldsymbol{\lambda}(t)}{dt} \right]^T \cdot \delta \mathbf{y}(t) \right. \\
& \left. + [\mathbf{a}(\mathbf{y}(t), \mathbf{c}_d, t) - \dot{\mathbf{y}}(t)]^T \cdot \delta \boldsymbol{\lambda}(t) + \left[\frac{\partial (\boldsymbol{\lambda}^T(t) \cdot \mathbf{a}(\mathbf{y}(t), \mathbf{c}_d, t))}{\partial \mathbf{c}_d} \right]^T \cdot \delta \mathbf{c}_d \right] dt
\end{aligned} \tag{A.12}$$

Taking the first three variations as arbitrary results in the following three differential equations and boundary conditions to be satisfied

$$\begin{aligned}
\boldsymbol{\lambda}(t_f) &= \frac{\partial g(\mathbf{y}(t_f))}{\partial \mathbf{y}} \\
\frac{d\boldsymbol{\lambda}(t)}{dt} &= - \frac{\partial}{\partial \mathbf{y}} (\boldsymbol{\lambda}^T(t) \cdot \mathbf{a}(\mathbf{y}(t), \mathbf{c}_d, t)) \\
\dot{\mathbf{y}}(t) &= \mathbf{a}(\mathbf{y}(t), \mathbf{c}_d, t)
\end{aligned} \tag{A.13}$$

The multiplier of the variation $\delta \mathbf{c}_d$ will yield the expression for the evaluation of the gradient $\nabla_{\mathbf{c}_d} g(\mathbf{y}(t_f))$. This expression becomes

$$\delta J_a = \frac{\partial J_a}{\partial \mathbf{c}_d} \cdot \delta \mathbf{c}_d \Rightarrow \frac{\partial J_a}{\partial \mathbf{c}_d} = \int_{t_o}^{t_f} \frac{\partial (\boldsymbol{\lambda}^T(t) \cdot \mathbf{a}(\mathbf{y}(t), \mathbf{c}_d, t))}{\partial \mathbf{c}_d} dt \tag{A.14}$$

which is the desired gradient since

$$\begin{aligned}
\nabla_{\mathbf{c}_d} g(\mathbf{y}(t_f)) &= \frac{\partial}{\partial \mathbf{c}_d} [g(\mathbf{y}(t_f))] = \\
&= \frac{\partial}{\partial \mathbf{c}_d} \left[\int_{t_o}^{t_f} \left[\left[\frac{dg(\mathbf{y}(t))}{d\mathbf{y}}(\mathbf{y}(t)) \right]^T \cdot \dot{\mathbf{y}} \right] dt + g(\mathbf{y}(t_o)) \right] \equiv \frac{\partial J_a}{\partial \mathbf{c}_d} \Big|_{\mathbf{a}(\mathbf{y}(t), \mathbf{c}_d, t) - \dot{\mathbf{y}}(t) = \mathbf{0}}
\end{aligned} \tag{A.15}$$

For the constraint in Eq. (17), the vector \mathbf{y} is $\mathbf{y} = \{\mathbf{E}_h^T \mathbf{d}_{m,p}^T \mathbf{x}^T \mathbf{v}^T \mathbf{f}_h^T\}^T$, the constraint, $g(\mathbf{y}(t_f))$, is

$$g(\mathbf{y}(t_f)) = \frac{\mathbf{1}^T \cdot \mathcal{D}^{q+1}(\mathbf{E}_h(t_f)) \cdot \mathbf{1} + \mathbf{1}^T \cdot \mathcal{D}^p(\mathbf{d}_{m,p}(t_f)) \cdot \mathbf{1}}{\mathbf{1}^T \cdot \mathcal{D}^q(\mathbf{E}_h(t_f)) \cdot \mathbf{1} + \mathbf{1}^T \cdot \mathcal{D}^p(\mathbf{d}_{m,p}(t_f)) \cdot \mathbf{1}} \tag{A.16}$$

the function $\mathbf{a}(\mathbf{y}(t), \mathbf{c}_d, t)$ is

$$\mathbf{a}(\mathbf{y}(t), \mathbf{c}_d, t) = \left\{ \begin{array}{l} \mathcal{D}^{-1}(\mathbf{E}_h^{all}) \cdot \mathcal{D}(\mathbf{f}_h(t)) \cdot (\mathbf{B}_{xf} \mathbf{v}(t)) \\ \frac{1}{t_f} (\mathcal{D}^{-1}(\mathbf{d}^{all}) \cdot \mathcal{D}(\mathbf{H}_x \cdot \mathbf{x}(t)))^p \cdot \mathbf{1} \\ \mathbf{v}(t) \\ \mathbf{M}^{-1}(-[\mathbf{C} + \mathbf{C}_d(\mathbf{c}_d)] \cdot \mathbf{v}(t) - \mathbf{K}_\alpha \mathbf{x}(t) - \mathbf{B}_{fx} \mathbf{f}_h(t) - \mathbf{M} \cdot \mathbf{e} \cdot \mathbf{a}_g(t)) \\ \mathbf{f}(\mathbf{v}(t), \mathbf{f}_h(t)) \end{array} \right\} \quad (\text{A.17})$$

and the vector λ is given by

$$\lambda = \{\lambda_{Eh}^T \quad \lambda_{dmp}^T \quad \lambda_x^T \quad \lambda_v^T \quad \lambda_{fh}^T\}^T \quad (\text{A.18})$$

Substituting Eqs. (A.16)-(A.18) to Eq. (A.14) yields the gradient of the constraint in Eq. (17), which is

$$\nabla_{\mathbf{c}_d} pi(\mathbf{c}_d) = - \int_{t_o}^{t_f} \mathbf{v}^T(t) \cdot \frac{\partial \mathbf{C}_d^T(\mathbf{c}_d)}{\partial \mathbf{c}_d} \cdot \mathbf{M}^{-T} \cdot \lambda_v \, dt \quad (\text{A.19})$$

The set of differential equations and boundary conditions are attained by substituting Eqs. (A.16)-(A.18) to Eq. (A.13) to yield

$$\begin{aligned} \lambda_{Eh}(t_f) &= \frac{1}{den^2} (den \cdot (q+1) \cdot \mathcal{D}^q(\mathbf{E}_h(t_f)) \cdot \mathbf{1} - num \cdot (q) \cdot \mathcal{D}^{q-1}(\mathbf{E}_h(t_f)) \cdot \mathbf{1}) \\ \lambda_{dmp}(t_f) &= \frac{1}{den^2} \left(den \cdot \left(\frac{q+1}{p} \right) \cdot \mathcal{D}^{\left(\frac{q+1}{p} - 1 \right)}(\mathbf{d}_{m,p}(t_f)) \cdot \mathbf{1} - num \cdot \left(\frac{q}{p} \right) \cdot \mathcal{D}^{\left(\frac{q}{p} - 1 \right)}(\mathbf{d}_{m,p}(t_f)) \cdot \mathbf{1} \right) \end{aligned} \quad (\text{A.20})$$

$$\lambda_x(t_f) = \mathbf{0}$$

$$\lambda_v(t_f) = \mathbf{0}$$

$$\lambda_{fh}(t_f) = \mathbf{0}$$

$$\dot{\lambda}_{Eh}(t) = \mathbf{0}$$

$$\dot{\lambda}_{dmp}(t) = \mathbf{0}$$

$$\dot{\lambda}_x(t) = (\mathbf{M}^{-1} \cdot \mathbf{K}_\alpha)^T \cdot \lambda_v(t) + \left(-p \frac{1}{t_f} \mathbf{H}_x^T \cdot \mathcal{D}^{p-1}(\mathbf{H}_x \cdot \mathbf{x}(t)) \mathcal{D}^{-p}(\mathbf{d}^{all}) \cdot \lambda_{dmp}(t) \right) \quad (\text{A.21})$$

$$\begin{aligned} \dot{\lambda}_v(t) &= -\lambda_x(t) + (\mathbf{M}^{-1} \cdot [\mathbf{C} + \mathbf{C}_d(\mathbf{c}_d)])^T \cdot \lambda_v(t) - \left(\frac{\partial \mathbf{f}(\mathbf{v}(t), \mathbf{f}_h(t))}{\partial \mathbf{v}} \right)^T \cdot \lambda_{fh}(t) + \\ &\quad + (-\mathbf{B}_{xf}^T \cdot \mathcal{D}(\mathbf{f}_h(t)) \cdot \mathcal{D}^{-1}(\mathbf{E}_h^{all}) \cdot \lambda_{Eh}(t)) \end{aligned}$$

$$\begin{aligned}
\dot{\lambda}_{fh}(t) &= (\mathbf{M}^{-1} \cdot \mathbf{B}_{fx})^T \cdot \lambda_v(t) - \left(\frac{\partial \mathbf{f}(\mathbf{v}(t), \mathbf{f}_h(t))}{\partial \mathbf{f}_h} \right)^T \cdot \lambda_{fh}(t) + \\
&\quad + \left(-\mathcal{D}(\mathbf{B}_{xf} \cdot \mathbf{v}(t)) \cdot \mathcal{D}^{-1}(\mathbf{E}_h^{all}) \cdot \lambda_{Eh}(t) \right) \\
\dot{\mathbf{E}}_h(t) &= \mathcal{D}^{-1}(\mathbf{E}_h^{all}) \cdot \mathcal{D}(\mathbf{f}_h(t)) \cdot (\mathbf{B}_{xf} \mathbf{v}(t)) ; \mathbf{E}_h(0) = \mathbf{0} \\
\dot{\mathbf{d}}_{m,p} &= \frac{1}{t_f} \left(\mathcal{D}^{-1}(\mathbf{d}^{all}) \cdot \mathcal{D}(\mathbf{H}_x \cdot \mathbf{x}(t)) \right)^p \cdot \mathbf{1} ; \mathbf{d}_{m,p}(0) = \mathbf{0} \\
\dot{\mathbf{x}}(t) &= \mathbf{v}(t) ; \mathbf{x}(0) = \mathbf{0} \\
\dot{\mathbf{v}}(t) &= \mathbf{M}^{-1} \left(-[\mathbf{C} + \mathbf{C}_d(\mathbf{c}_d)] \cdot \mathbf{v}(t) - \mathbf{K}_\alpha \mathbf{x}(t) - \mathbf{B}_{fx} \mathbf{f}_h(t) - \mathbf{M} \cdot \mathbf{e} \cdot \mathbf{a}_g(t) \right) ; \mathbf{v}(0) = \mathbf{0} \\
\dot{\mathbf{f}}_h(t) &= \mathbf{f}(\mathbf{v}(t), \mathbf{f}_h(t)) ; \mathbf{f}_h(0) = \mathbf{0}
\end{aligned} \tag{A.22}$$

where *num* and *den* are given by

$$\begin{aligned}
num &= \mathbf{1}^T \cdot \mathcal{D}^{q+1}(\mathbf{E}_h(t_f)) \cdot \mathbf{1} + \mathbf{1}^T \cdot \mathcal{D}^{\frac{q+1}{p}}(\mathbf{d}_{m,p}(t_f)) \cdot \mathbf{1} \\
den &= \mathbf{1}^T \cdot \mathcal{D}^q(\mathbf{E}_h(t_f)) \cdot \mathbf{1} + \mathbf{1}^T \cdot \mathcal{D}^{\frac{q}{p}}(\mathbf{d}_{m,p}(t_f)) \cdot \mathbf{1}
\end{aligned} \tag{A.23}$$

Eq. (A.22) return the equality constraints; Eqs. (A.20) and (A.21) give expressions for the evaluation of the Lagrange multipliers λ_x , λ_v and λ_{dmp} which are needed for the evaluation of Eq. (A.19). Now since the elements of $\mathbf{C}_d^T(\mathbf{c}_d)$ are linear combinations of the elements of \mathbf{c}_d , the differentiation of $\mathbf{C}_d^T(\mathbf{c}_d)$ with respect to $\mathbf{c}_{d,i}$ (also needed in Eq. (A.19)) is rather simple and easily programmed.

The computation of the gradient for a single record is summarized as follows:

Stage 1: Solve the equations of motion (Eq. (A.22)).

Stage 2: Solve the equations of the Lagrange multipliers (Eq. (A.21)) with the final conditions in Eq. (A.20)).

Stage 3: Calculate the desired gradient (Eq (A.19)).